J. Electrochem. Sci. Eng. **13(5)** (2023) 783-793; http://dx.doi.org/10.5599/jese.1623

Open Access : : ISSN 1847-9286
www.jESE-online.org

Original scientific paper

Electrode configurations study for alkaline direct ethanol fuel cells

Michaela Roschger[1,✉], Sigrid Wolf[1], Andreas Billiani[1], Selestina Gorgieva[2], Boštjan Genorio[3] and Viktor Hacker[1]

[1]*Institute of Chemical Engineering and Environmental Technology, Graz University of Technology, Inffeldgasse 25/C, 8010 Graz, Austria*
[2]*Faculty of Mechanical Engineering, University of Maribor, Smetanova ulica 17, 2000 Maribor, Slovenia*
[3]*Faculty of Chemistry and Chemical Technology, University of Ljubljana, Večna pot 113, 1000 Ljubljana, Slovenia*

Corresponding author: ✉michaela.roschger@tugraz.at

Received: November 29, 2022; Accepted: March 24, 2023; Published: March 28, 2023

Abstract

The direct electrochemical conversion of ethanol, a sustainable fuel, is an alternative sustainable technology of the future. In this study, membrane electrode assemblies with different electrode configurations for an alkaline direct ethanol fuel cell were fabricated and tested in a fuel cell device. The configurations include a catalyst-coated substrate (CCS), a catalyst-coated membrane (CCM), and a mixture of these two fabrication options. Two different anion exchange membranes were used to perform a comprehensive analysis. The fabricated CCSs and CCMs were characterized with single cell measurements, electrochemical impedance spectroscopy and scanning electron microscopy. In addition, the swelling behavior of the membranes in alkaline solution was investigated in order to obtain information for CCM production. The results of the experimental electrochemical tests show that the CCS approach provides higher power densities (42.4 mW cm^{-2}) than the others, regardless of the membrane type.

Keywords

Membrane electrode assembly; alkaline swelling; single cell tests; anion exchange membrane

Introduction

Alternative, sustainable, and environmentally friendly technologies are receiving a tremendous amount of attention due to the growing environmental awareness of the human population as a result of global warming. Energy conversion devices such as fuel cells represent promising alternatives to fossil fuel-powered devices and can ensure a significant contribution to the

production of energy from renewable sources. The most heavily researched fuel cell today is the proton-exchange membrane fuel cell (PEMFC), but the anion exchange membrane fuel cell (AEMFC) is also regaining importance. These two types differ in terms of the electrolyte or membrane used: The PEMFC uses a cation exchange membrane, and the AEMFC uses an anion exchange membrane (AEM) [1,2]. Another important difference is that AEMFC can use inexpensive, non-noble metal catalysts, while PEMFC must use the costly and scarce catalyst platinum [3-6].

A special form of AEMFC is the alkaline direct ethanol fuel cell (DEFC), shown in Figure 1. This fuel cell allows the use of ethanol as a fuel, which has advantages associated with its renewability, liquid state (convenient handling and storage), low toxicity, and high energy density (8 kWh kg^{-1}) [1,5,6].

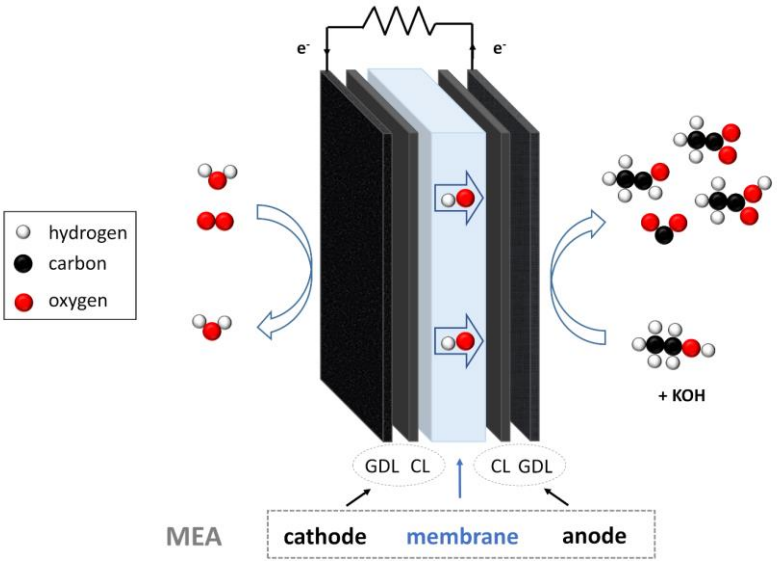

Figure 1. *Working principle (reactants + products) of an alkaline DEFC (CL: catalyst layer; GDL: gas diffusion layer, MEA: membrane electrode assembly)*

However, the use of this fuel also presents challenges, such as the fact that ethanol is incompletely converted on the anode side. No catalysts have been identified that fully perform the ethanol oxidation reaction (EOR). Instead of splitting ethanol completely to CO_2 and 12 e^-, acetate (acetic acid) or acetaldehyde and thereby less electrons are formed. The research on EOR catalysts is focused on Pt- or Pd-based catalysts, whereby Pd catalysts show four times higher performance than Pt catalysts in alkaline media. The combination of less expensive ad-atoms like Ag, Ru, Co, Fe or Ni with Pd-catalysts to produce bi- or tri-metallic catalysts can further enhance the activity of the catalysts [5,7-11].

In AEMFCs, *e.g.* commercial AEMs based on synthetic polymers with quaternary ammonium groups (Fumatech, Solvay, Japan Tokuyama Corporation) and membranes with polysaccharide-based biomaterials like chitosan (CS) can be used [4]. The use of AEMs in alkaline fuel cells compared to liquid-electrolyte systems exhibit a lower fuel crossover rate and an improved CO_2 tolerance [2]. However, these can swell in aqueous solutions and become brittle under dry storage conditions after undergoing anionic conversion in KOH; and must therefore kept hydrated afterwards [2]. Moreover, there are other challenges to cope with AEM utilization, such as the thermal and mechanical stability, and the ionic conductivity [2,5,12]. In order to increase the ionic conductivity inside the cell and to improve the EOR performance, an alkaline solution (KOH) is added to the fuel [2,4,5,13]. The addition of KOH, and therefore OH^- ions, in the AEMFC also has a conflicting adverse effect, which is long term degradation, by nucleophilic attack or Hoffman elimination reaction [2]. Furthermore, the addition of alkaline solution, unfortunately has also a big drawback in the alkaline DEFC: possible produced CO_2

can react with the OH^- ions and form carbonate or bicarbonates and further carbonate salts (in case of KOH: K_2CO_3). The produced carbonate salts can block the pores of the catalyst layer and precipitate on the membrane [1,7]. Despite these disadvantages, the addition of alkaline solution increases the power output of alkaline fuel cells; the advantages predominate over the disadvantages at least in short term [1]. Due to the use of the liquid fuel, the gas diffusion layer (GDL) requirements on the anode side of the cell differ from those on the cathode side (hydrophilic vs. hydrophobic). The GDL should provide the best possible diffusion medium for ethanol, and the literature shows that the use of a carbon cloth as a GDL is ideal [14,15].

The electrodes (i.e., the catalyst layer (CL) and GDL) and the membrane together form the membrane electrode assembly (MEA), which represents the heart of a fuel cell. The MEA can be manufactured with one of this two basic methods, namely, using catalyst-coated substrates (CCS) or catalyst-coated membranes (CCM). With the first option, the catalyst ink is applied to the GDL substrate, and the resulting CCSs or gas diffusion electrodes (GDEs) are connected to the membrane. With the second option, the ink is applied to the membrane, and the resulting CCMs are connected together with the blank GDLs [16-18]. Several ways to apply the catalyst ink have been reported, such as blading, spraying, or printing, whereby spraying has found to be suitable on a laboratory scale [16-20].

There are studies on the production methods of the whole MEA related to acidic DEFC, but nearly no studies for the alkaline DEFC. Song *et al.* [18]. proved that the catalyst layer containing Nafion solution can be delaminated in the acidic DEFC as a result of Nafion® 115 membrane swelling in ethanol solution. Moreno-Jiménez *et al.* [17] showed that a combination of the inner and outer catalyst layer (*i.e.* on GDL and membrane: Nafion® 117) in the acidic DEFC positively effects cell performance, due to lower ohmic resistances. However, in the acidic DEFC, no additional KOH is added; therefore, the conditions differ from those in the alkaline DEFC. Several studies have been performed on fabrication optimization for alkaline electrolysis with anion exchange membranes. For example, Plevová *e- i.* [21] developed a membrane and ionomer for the alkaline water electrolyzer which can be used to produce with a computer-controlled ultrasonic dispersion deposition method CCMs. Ito *et al.* [20] discovered that the CCM-cathode and CCS-anode is the most appropriate configuration when using commercial membranes.

Considering this background, the aim of this study was to investigate the influence of the electrode configuration in the MEA on the performance of the liquid feed alkaline DEFC, since the properties of this type of fuel cell (liquid KOH and AEMs) are challenging. Three different electrode configurations with both commercially available and custom-made AEMs were used in this work: (a) configuration A with a GDE-based MEA, (b) configuration B with a CCM-based MEA, and (c) configuration C with a mixture of CCM and GDE. The produced MEAs were characterized electrochemically in a single cell. Furthermore, the morphological features of the MEAs were characterized with scanning electron microscopy (SEM). In addition, the swelling behavior of the membranes in the alkaline solutions used was investigated.

Experimental

Materials

The following materials and chemicals were used without further purification: Ethanol (EtOH, 99.9 % *p.a.*), potassium hydroxide (KOH ≥ 85 %, *p.a.*, pellets) and 2-propanol (99.9 % *p.a.*) were purchased by Carl Roth (Karlsruhe, Germany). Carbon cloth (ELAT - Hydrophilic Plain Cloth, 0.406 mm thick) and carbon paper (Sigracet 29 BC, 0.235 mm thick) were delivered from fuel cell store (College

Station, TX, USA). Fumasep® FAA-3-50 (anion-exchange membrane, non-reinforced, 50 µm) and Nafion™ Solution (NS-5, PFSA 5%,) were purchased from Fumatech (Bietigheim-Bissingen, Germany) and Quintech (Göppingen, Germany), respectively. A CS/N-rGONRs anion exchange membrane (0.07 % N-rGONRs) that was previously developed was used [4]. An Ag-Mn_xO_y/C cathode catalyst, as well as a PdNiBi/C anode catalyst, both consisting of 30 wt.% catalytic active material on the support material Vulcan, as previously reported were utilized [8,11]. Ultrapure water (~18 MΩ cm, Barnstead NANOpure-Water Purification system (Dubuque, IA, USA)) was used for the preparation of the solutions and inks.

MEA configurations

The utilized spray-coated MEA configurations are shown in Figure 2. Configurations consisting of a CCS + CCS (configuration A), a CCM + CCM (configuration B), and a mixture of these two (CCM_{anode} + + $CCS_{cathode}$ = configuration C) were tested. The membranes selected comprised two different AEMs, the CS/N-rGONRs [4] and the commercial fumasep® FAA-3-50 membrane. Configuration A and B were tested with both membranes, whereas configuration C was only tested with the CS/N-rGONRs membrane. The MEAs were obtained by assembling the individual parts together depending on the configuration.

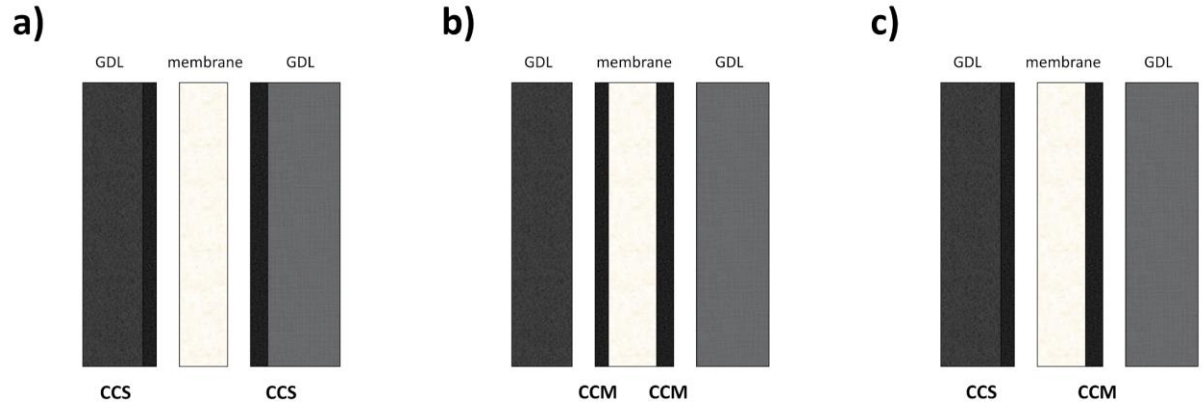

Figure 2. *Schematics of different electrode configurations used for MEA production (anode right and cathode left) (a) configuration A, (b) configuration B and (c) configuration C*

Ink formulation and preparation

The catalyst ink for the spray-coating process and thus the preparation of CCSs or CCMs consisted of the respective catalyst (Ag-Mn_xO_y/C for cathode and PdNiBi/C for anode), isopropanol, water and Nafion-ionomer (binder) solution, whereby the catalyst mass concentration was 4 mg mL^{-1}. Nafion ionomer was used because commercial anion exchange ionomers still have low thermal and chemical stability [5], and the addition of the aqueous fuel or humidified oxygen enables Nafion to be used [22]. The ratio of water to isopropanol was 7:3 and the amount of ionomer/binder in the solution was 30 wt.% of the catalyst mass. All produced electrodes featured an I/C (ionomer/carbon) ratio of 0.6. To obtain a homogeneous dispersion, the mixture was ultrasonicated using an ultrasonicbath.

Coating conditions

The CCSs were prepared by spraying the catalyst inks on the GDLs, whereby the carbon cloth was utilized at the anode and carbon paper on the cathode, using an ultrasonic Sonotech ExactaCoat OP3 spray coater (SonoTek Corporation, USA) with a 120 kHz nozzle. The GDLs were fixed on a porous PTFE substrate, which was tempered to 80 °C, using a template to spray a surface area of 4 cm^2. The nozzle was continuously moved back and forth and from left to right and vice versa in staggered serpentine

lines at a constant height of approximately 6 cm during the spraying process in an automated manner in order to obtain a homogeneous, uniform coating. An anodic active material loading of 0.5 mg cm^{-2} and a cathodic active material loading of 0.25 mg cm^{-2} were applied [8].

The same procedure was used to produce the CCMs, but the dry membrane was coated instead. To prevent the membrane from wrinkling during the spray process, it was additionally fixed by vacuum suction.

Anionic conversion and KOH doping of the membranes

The pure membranes, as well as the CCMs, were pretreated in de-aerated 1 M KOH for 24 h [4]. Commercial AEMs are normally stored in the stable Cl^-/Br^- form; therefore, they require anionic conversion to be present in the OH^- form. A special fixture was used to clamp the CCMs. The membrane cannot be converted or doped with KOH before applying the catalyst with the spray coater to it, since it would dry out and become brittle [2].

Another configuration B variant of the CS/N-rGONRs membrane (configuration B_{II}) was produced, which was incorporated dry into the cell without KOH doping of the membrane outside the cell; however, the membrane was doped inside, to see if fixation with the flow fields had an influence on the results. For this purpose, the test rig [13] was adapted by purging with N_2 (1 mL min^{-1}) through the cathode side and passing a 1 M KOH solution (0.3 mL min^{-1}) through the anode side for 24 h. The low flow rates were selected to optimally mimic the KOH doping of the other configuration B variant for comparison.

Membrane characteristics in alkaline (ethanol) solution

The swelling rate of the two AEMs was evaluated in 1 M KOH at RT after 24 h (swelling during anionic conversion and doping with KOH) and afterwards after 1 h and 24 h in a mixture of 1 M KOH and 1 M EtOH solution. Therefore, the in-plane and through-plane dimensions were measured at the given time intervals and the change calculated.

Single cell tests

All single cell tests of the prepared MEAs were conducted with a IM6ex potentiostat combined with a PP240 power potentiostat (Zahner-elektrik GmbH & Co. KG, Germany) and utilizing a self-designed cell [13]. In these tests, after heating up the cell and purging with highly basic solution and oxygen, the current was ramped up from small (~0.4 mA cm^{-2}) to high current densities using a step time of 30s, and the cell voltage was recorded until a cell potential of 0.180 V was reached. These performance tests were conducted with continuous supply of a liquid mixture of 1 M KOH and 1 M EtOH at a flow rate of 5 mL min^{-1} at the anode side and with humidified oxygen (60 % RH) at a flow rate of 25 ml min^{-1} at the cathode side of the cell. The measurements were performed at 80 °C.

In addition to the polarization curves, electrochemical impedance spectra (EIS) of configuration A and configuration C (both CS/N-rGONRs membrane) at 440 mA (amplitude: 10 %) between 50 kHz and 0.1 Hz were recorded after 5 min stabilization time. For fitting and evaluation, the equivalent circuit model from previous work [13] and ZView® software (Scribner Associates Inc., Southern Pines, NC, USA) was applied.

Scanning electron microscopy

The SEM images of the catalyst layers on the different membranes and electrodes were recorded with a Zeiss ULTRA plus using Inlens and SE2 detectors at 2 kV or 5 kV at WD 5.5 mm by adhering the samples to an aluminum holder with conductive carbon tape.

Results and discussion

In this section, the results of the membrane swelling characteristics (in KOH and a mixture of KOH and EtOH) are discussed first. The obtained behavior characteristics of the membranes were used to declare the influence of the MEA production process on the performance in the single cell. EIS measurements were applied to point out the impact of the electrode configuration on resistance. Moreover, specific photos and SEM images were shown to support the results.

Membrane characteristics in alkaline (ethanol) solution

The swelling behavior of membranes is an important issue for the production and performance of CCMs, due to possible delamination of the catalyst layer [18]. In Figure 3 a, the in-plane and through-plane swelling in 1 M KOH after 24 h, thus the swelling during anionic conditioning or KOH doping, can be seen. The custom-made CS/N-rGONRs AEM undergoes an in-plane change of 15 %, whereas the through-plane swelling of 78 % is very high. The FAA-3-50 membrane behaves in exactly the opposite way, changing in-plane by 26 % and through-plane only by 2 %. However, this means that both membranes change significantly in size (CS/N-rGONRs changes considerably more) over the measured time period, resulting in a thickness of 55.7 ± 0.9 µm for the FAA-3-50 and 57.0 ± 0.8 µm for the CS/N-rGONRs.

For the investigation of the membrane swelling behavior during the measurement, the size change in 1 M KOH and 1 M EtOH was studied (Figure 3 b). The remarkable result obtained is that the through-plane swelling behavior is constant for both membranes between 1 h and 24 h. In other words, both membranes swell in thickness to a certain degree (CS/N-rGONRs: 11 % and FAA-3-50: 4 %) and then remain unchanged. However, both membranes enlarge in-plane over time, but the FAA-3-50 (1h: 8 % and 24 h: 25 %) more than the CS/N-rGONRs (1h: 0 % and 24 h: 2 %). Thus, the swelling behavior of the membranes is comparable to the swelling behavior in 1 M KOH: the CS/N-rGONRs swells more through-plane, and FAA-3-50 more in-plane. The total size change of the membranes after 24 h in 1 M KOH and 24 h in 1 M KOH and 1 M EtOH results in an in-plane swelling of 18 and 57 % for the CS/N-rGONRs and the FAA-3-50, respectively and a through-plane swelling of 98 and 5 % for the CS/N-rGONRs and the FAA-3-50, respectively.

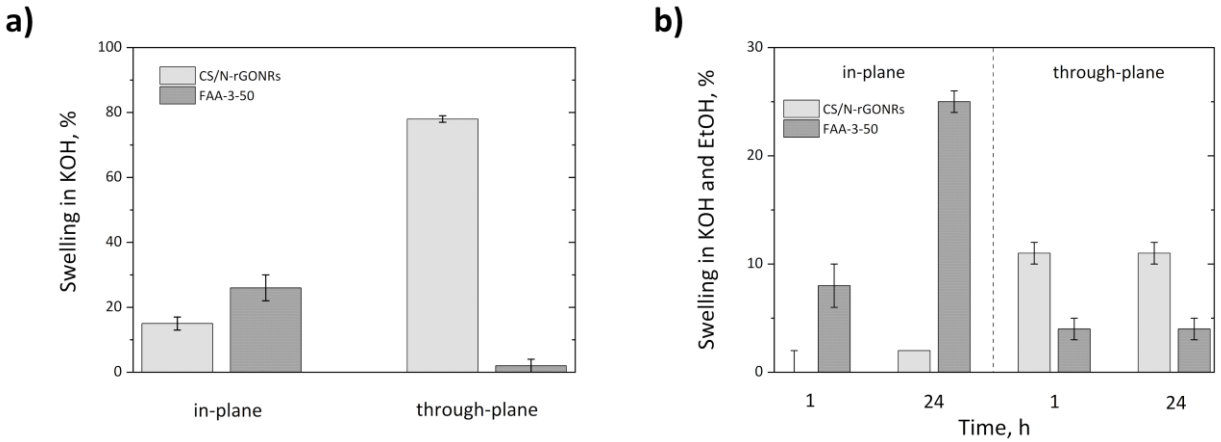

Figure 3. *Membrane swelling in (a) 1 M KOH solution after 24 h and (b) in a mixture of 1 M EtOH and 1 M KOH solution*

Single cell tests

The influence of the electrode configuration in the MEA on the performance in the single cell can be seen in Figure 4.

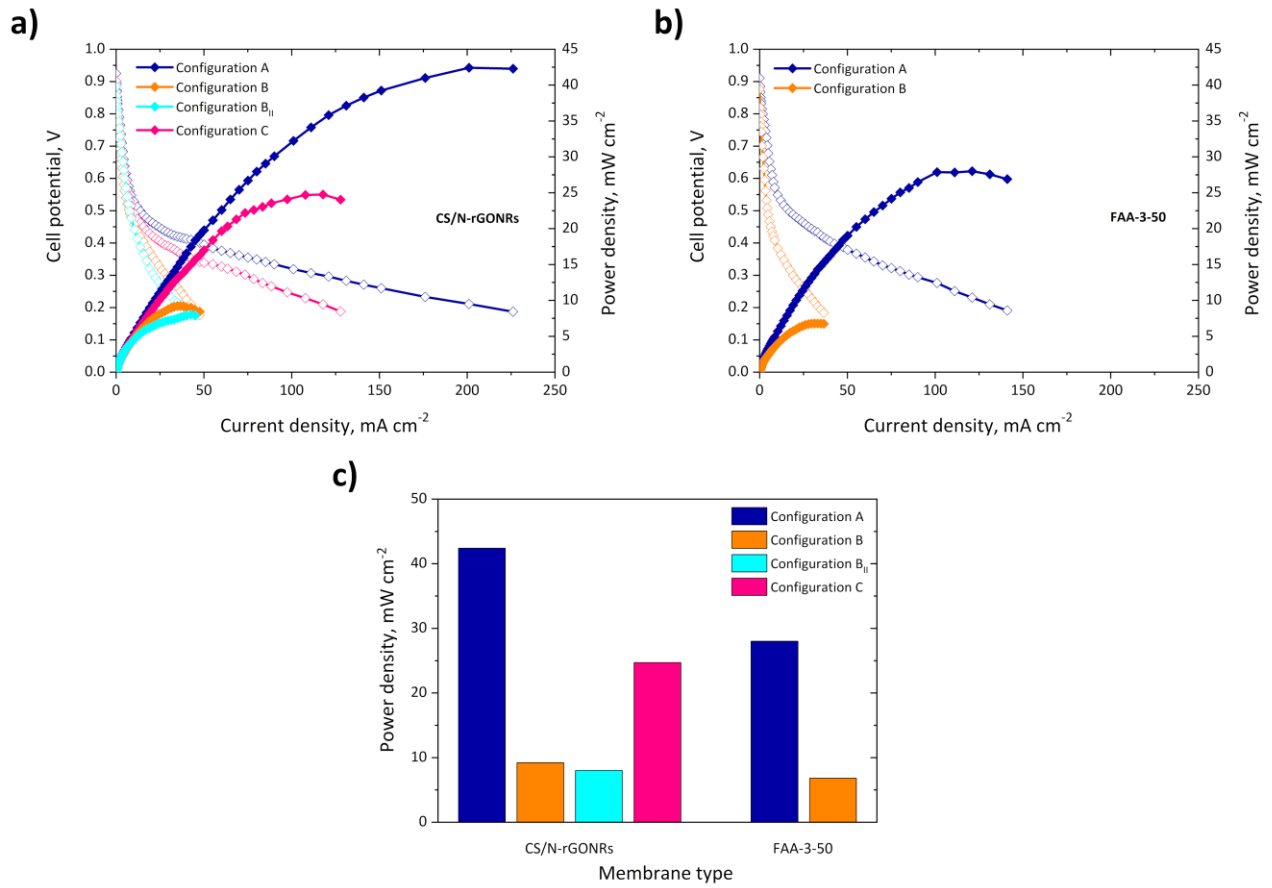

Figure 4. *Polarization and power density curves of the electrode configurations for the different membranes (a) CS/N-rGONRs, (b) fumasep® FAA-3-50, and (c) bar chart of the power densities obtained for all measurements*

The configuration A approach yielded the highest power densities for both membranes used, whereby configuration B always performed worse. However, the difference between the values obtained for configuration A and configuration B for the tested membranes is considerable. The performance of configuration B is only one-fifth of the configuration A performance with the CS/N-rGONRs AEM (9.2 mW cm^{-2} *vs.* 42.4 mW cm^{-2}). The performance seen with the commercially available fumasep® FAA-3-50 AEM, meanwhile, was only one-fourth of the latter (6.8 mW cm^{-2} *vs.* 28.0 mW cm^{-2}). A clear trend is visible, *i.e.* that the power losses are lower for the commercial membrane due to their swelling behavior during anionic conversion, as shown before. The high through-plane swelling of the CS/N-rGONRs AEM resulted in large cracks in the catalyst layer, if the catalyst layer was sprayed on the membrane. Smaller cracks were also seen within the FAA-3-50 membrane, due to the in-plane swelling. However, the maximum power density values are still lower than those of the custom-made membrane.

The performance of the configuration B_{II} variant (where the doping with KOH of the membrane was performed inside of the cell) of the CS/N-rGONRs AEM was even lower (8.0 mW cm^{-2}) than that of configuration B. This is due to the fact that the configuration B_{II} type did not undergo full KOH doping. Only the active surface (where the catalyst layer is located) of the MEA was in contact with KOH at the anode (through the flow field). The whole membrane of the configuration B variant, however, was completely exposed to KOH.

Configuration C resulted in much better performance (24.7 mW cm^{-2}) than configuration B, but worse (one-half) than configuration A. For the investigation of this power loss, configuration A and configuration C were analyzed with EIS (Figure 5) to determine their resistances. The electrolyte

resistance R_{el} (membrane) is nearly the same for both configurations, but a little bit higher for configuration C. The anodic ionomer resistance $R_{ion,a}$, the charge transfer resistance $R_{ct,a}$ and the mass transfer resistance R_{mt} and the resulting overall resistance R_{ges} increased for configuration C. Therefore, the interface or connection of GDE and membrane in comparison to GDL and CCM is preferable, due to lower ohmic resistance, as a result of lower ionic repulsion between the sulfonated groups of the ionomer and the hydroxide anions. Possible presence of water at the interface between the membrane and the GDE favors hydroxide transport [23].

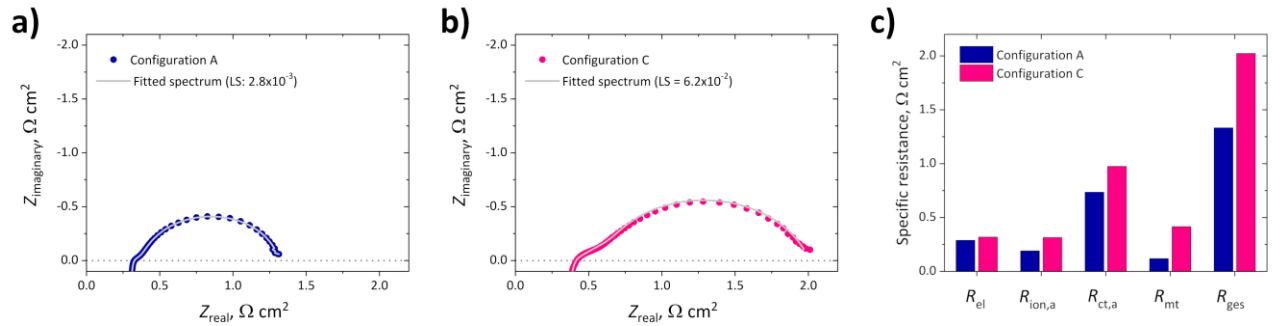

Figure 5. *Electrochemical impedance spectra of (a) configuration A, (b) configuration C, and (c) bar chart of the resistances of the CS/N-rGONRs AEM measurements*

Thus, the double CCS configuration had a clear advantage among both membranes which are anionic converted or KOH doped in the alkaline DEFC for cell measurement. The more CCS configurations were replaced by CCM, the worse the performance was due to higher resistances.

Visual investigation of the different electrode configurations

The different electrode configurations of the CS/N-rGONRs membrane were visually investigated before and after the single cell tests and the results are illustrated in photos. In Figure 6 a the configuration B of the CS/N-rGONRs AEM can be seen after 24 h KOH doping.

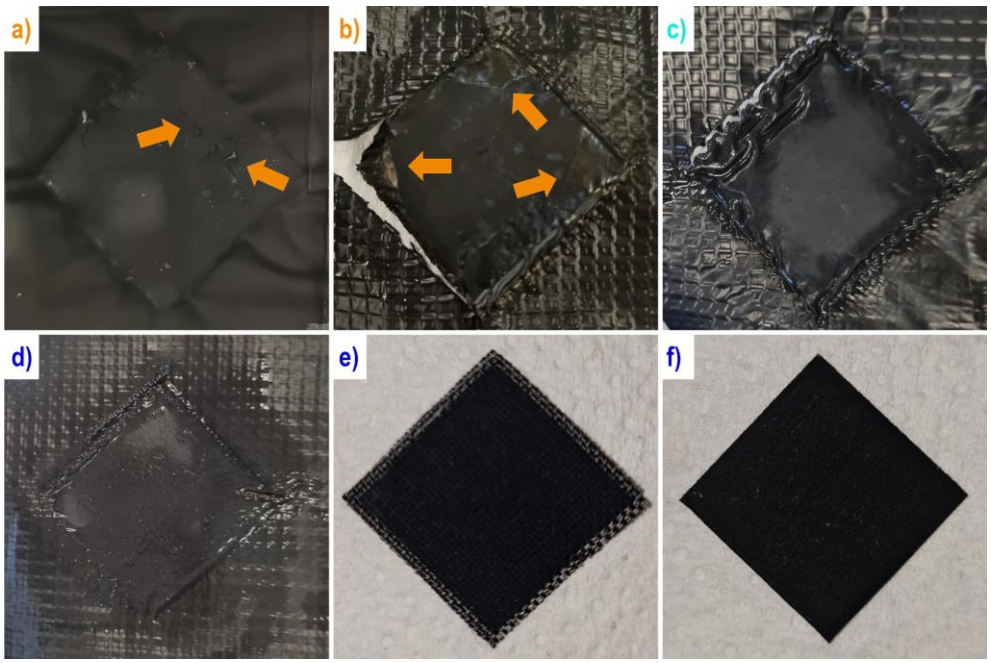

Figure 6. *Photographs of the different electrode configurations before and after single cell testing (a) configuration B before, (b) configuration B after, (c) configuration B_{II} after, (d) configuration A after, (e) configuration A anodic GDE after, and (f) configuration A cathodic GDE after*

After immersion in KOH, cracks can be seen in the catalyst layer, due to the swelling of the CS/N-rGONRs AEM, which could not be prevented [4], as determined before. These are even more pronounced after the cell measurement and delamination of the catalyst layer from the membrane can be seen in Figure 6 b (the visible crack in the membrane occurred after the measurement during cell disassembly by taking off from the gasket). The cubic pattern exterior the active MEA area is due to the gasket used inside the cell to prevent leakage. However, it can be ruled out that the appearance of the larger and more pronounced cracks is due to the cell operation with the mixture of KOH and EtOH and membrane swelling in this solution, since no cracks are visible in Figure 6 c of configuration B_{II}. The pre-damage of immersion in KOH is the reason for these large cracks in configuration B. Configuration B_{II} was KOH doped within the cell under fixation of the flow field plates. In other words, the fixation counteracts swelling within the cell, regardless of whether KOH or a mixture of EtOH and KOH are used, since the catalyst layer is not damaged. This means, in turn, that we assume that delamination of the catalyst layer is caused by the membrane swelling behavior rather than by possible swelling of the ionomer/binder in the catalyst layer. These observations can also be seen in Figure 6 d-f. The membrane without catalyst layer is flat and planar and shows no visible swelling where the CCS was located (due to the fixation with the flow fields) and the catalyst layers on the substrates are not delaminated.

Scanning electron microscopy

The same observations could be made by performing SEM analyse of the catalyst layers on the membranes and substrates. In Figure 7 a and d no delamination of the catalyst layer from the GDLs can be seen. The marked cracks (blue arrows) in the catalyst layer result from the structure of the carbon paper, as shown in our previous work [11]. Configuration B can be seen in Figure 7 b and e, where a crack has formed in the catalyst layer on the left-hand side of the image. In contrast, as previously described, no cracks are visible in the catalyst layers of configuration B_{II} (Figure 7 c and f).

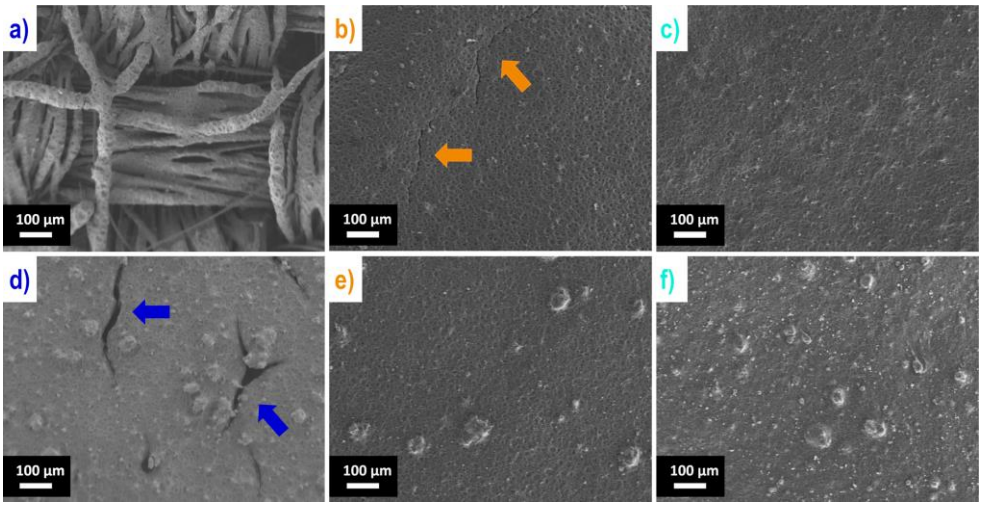

Figure 7. *SEM images of the catalyst layers after single cell testing (a and d) configuration A anode and cathode, (b and e) configuration B anode and cathode and (c and f) configuration B_{II} anode and cathode*

The photographic evidence indicates that AEM swelling and pretreatment is a major problem in the production of MEAs with CCMs [2]. Whereby the CCM variant is extremely useful, as a direct connection can be formed by applying the catalyst layer and the anion exchange ionomer on it, as shown in literature [20,21]. However, therefore research is needed to reduce membrane swelling during anionic conversion or doping with KOH and to develop chemically and thermally stable anion exchange ionomers [2].

Conclusions

The influence of the manufacturing method of the MEA with different membranes (commercially available and custom-made AEMs) could be successfully demonstrated. Due to the inevitable swelling of the AEMs during anionic conversion or KOH doping, the catalyst layer cracks; therefore, the CCM manufacturing method is currently not recommended for the tested AEMs in the alkaline DEFC using Nafion ionomer in the catalyst layer. Regardless of the membrane used, higher power densities could be achieved with the CCS fabrication variant on both sides (anode and cathode) than with the CCM variant. The cell resistance increases when the catalyst layer is applied to the membrane, which reduces the performance, due to the ionic repulsion between the sulfonated groups of the ionomer and the hydroxide anions.

***Acknowledgements**: The authors acknowledge the financial support from the Austrian Science Fund (FWF, grant number I 3871-N37) and Slovenian Research Agency (ARRS, grant number: N2-0087, P2-0118, and P1-0175) as part of the project »Graphene Oxide based MEAs for the Direct Ethanol Fuel Cell«. We also thank Azra Osmić for her help in producing the membranes and Kurt Mayer for his support in the evaluation of the EIS data.*

***Conflicts of Interest:** The authors declare no conflict of interest.*

References

[1] E. H. Yu, X. Wang, U. Krewer, L. Li, K. Scott. Direct oxidation alkaline fuel cells: From materials to systems, *Energy and Environmental Science* **5** (2012) 5668c5680. https://doi.org/10.1039/c2ee02552c

[2] T .B. Ferriday, P. H. Middleton. Alkaline fuel cell technology, *International Journal of Hydrogen Energy* **46** (2021) 18489-18510. https://doi.org/10.1016/j.ijhydene.2021.02.203

[3] S. Wolf, M. Roschger, B. Genorio, M. Kolar, D. Garstenauer, B. Bitschnau, V. Hacker. Ag-MnxOy on Graphene Oxide Derivatives as Oxygen Reduction Reaction Catalyst in Alkaline Direct Ethanol Fuel Cells, *Catalysts* **12** (2022) 780. https://doi.org/10.3390/catal12070780

[4] S. Gorgieva, A. Osmić, S. Hribernik, M. Božič, J. Svete, V. Hacker, S. Wolf, B. Genorio. Efficient chitosan/nitrogen-doped reduced graphene oxide composite membranes for direct alkaline ethanol fuel cells, *International Journal of Molecular Sciences* **22** (2021) 1740. https://doi.org/10.3390/ijms22041740

[5] T. S. Zhao, Y. S. Li, S. Y. Shen. Anion-exchange membrane direct ethanol fuel cells: Status and perspective, *Frontiers of Energy and Power Engineering in China* **4** (2010) 443-458. https://doi.org/10.1007/s11708-010-0127-5

[6] L. An, T. S. Zhao, Y. S. Li. Carbon-neutral sustainable energy technology: Direct ethanol fuel cells, *Renewable and Sustainable Energy Reviews* **50** (2015) 1462-1468. https://doi.org/10.1016/j.rser.2015.05.074

[7] L. Yaqoob, T. Noor, N. Iqbal. A comprehensive and critical review of the recent progress in electrocatalysts for the ethanol oxidation reaction, *RSC Advances* **11** (2021) 16768-16804. https://doi.org/10.1039/d1ra01841h

[8] M. Roschger, S. Wolf, K. Mayer, A. Billiani. Influence of the electrocatalyst layer thickness on alkaline DEFC performance, *Sustainable Energy and Fuels* **7** (2023) 1093-1106. https://doi.org/10.1039/d2se01729f

[9] B. Cermenek, B. Genorio, T. Winter, S. Wolf, J.G. Connell, M. Roschger, I. Letofsky-Papst, N. Kienzl, B. Bitschnau, V. Hacker. Alkaline Ethanol Oxidation Reaction on Carbon Supported Ternary PdNiBi Nanocatalyst using Modified Instant Reduction Synthesis Method, *Electrocatalysis* **11** (2020) 203-214. https://doi.org/10.1007/s12678-019-00577-8

[10] E. Antolini. Catalysts for direct ethanol fuel cells, *Journal of Power Sources* **170** (2007) 1-12. https://doi.org/10.1016/j.jpowsour.2007.04.009
[11] M. Roschger, S. Wolf, B. Genorio, V. Hacker. Effect of PdNiBi Metal Content : Cost Reduction in Alkaline Direct Ethanol Fuel Cells, *Sustainability* **14** (2022) 15485. https://doi.org/https://doi.org/10.3390/su142215485
[12] Z. Zakaria, S.K. Kamarudin, S.N. Timmiati. Membranes for direct ethanol fuel cells: An overview, *Applied Energy*. **163** (2016) 334-342. https://doi.org/10.1016/j.apenergy.2015.10.124
[13] M. Roschger, S. Wolf, K. Mayer, M. Singer, V. Hacker. Alkaline Direct Ethanol Fuel Cell : Effect of the Anode Flow Field Design and the Setup Parameters on Performance, *Energies* **15** (2022) 7234. https://doi.org/https://doi.org/10.3390/en15197234
[14] V. Alzate, K. Fatih, H. Wang. Effect of operating parameters and anode diffusion layer on the direct ethanol fuel cell performance, *Journal of Power Sources* **196** (2011) 10625-10631. https://doi.org/10.1016/j.jpowsour.2011.08.080
[15] P. Ekdharmasuit, A. Therdthianwong, S. Therdthianwong. Anode structure design for generating high stable power output for direct ethanol fuel cells, *Fuel* **113** (2013) 69-76. https://doi.org/10.1016/j.fuel.2013.05.046
[16] B. H. Lim, E. H. Majlan, A. Tajuddin, T. Husaini, W. R. Wan Daud, N. A. Mohd Radzuan, M. A. Haque. Comparison of catalyst-coated membranes and catalyst-coated substrate for PEMFC membrane electrode assembly, *Chinese Journal of Chemical Engineering* **33** (2021) 1-16. https://doi.org/10.1016/j.cjche.2020.07.044
[17] D. A. Moreno-Jiménez, D. E. Pacheco-Catalán, L. C. Ordóñez. Influence of MEA catalytic layer location and air supply on open-cathode direct ethanol fuel cell performance, *International Journal of Electrochemical Science* **10** (2015) 8808-8822. http://www.electrochemsci.org/papers/vol10/101108808.pdf
[18] S. Song, G. Wang, W. Zhou, X. Zhao, G. Sun, Q. Xin, S. Kontou, P. Tsiakaras. The effect of the MEA preparation procedure on both ethanol crossover and DEFC performance, *Journal of Power Sources* **140** (2005) 103-110. https://doi.org/10.1016/j.jpowsour.2004.08.011
[19] Z. Turtayeva, F. Xu, J. Dillet, K. Mozet, R. Peignier, A. Celzard, G. Maranzana. Manufacturing catalyst-coated membranes by ultrasonic spray deposition for PEMFC: Identification of key parameters and their impact on PEMFC performance, *International Journal of Hydrogen Energy* **47** (2022) 16165-16178. https://doi.org/10.1016/j.ijhydene.2022.03.043
[20] H. Ito, N. Miyazaki, S. Sugiyama, M. Ishida, Y. Nakamura, S. Iwasaki, Y. Hasegawa, A. Nakano. Investigations on electrode configurations for anion exchange membrane electrolysis, *Journal of Applied Electrochemistry* **48** (2018) 305-316. https://doi.org/10.1007/s10800-018-1159-5
[21] M. Plevová, J. Hnát, J. Žitka, L. Pavlovec, M. Otmar, K. Bouzek. Optimization of the membrane electrode assembly for an alkaline water electrolyser based on the catalyst-coated membrane, *Journal of Power Sources* **539** (2022) 231476. https://doi.org/10.1016/j.jpowsour.2022.231476
[22] Y. Liu, Z. Pan, O.C. Esan, X. Xu, L. An. Performance Characteristics of a Direct Ammonia Fuel Cell with an Anion Exchange Membrane, *Energy and Fuels* **36** (2022) 13203-13211. https://doi.org/10.1021/acs.energyfuels.2c02951
[23] P. Piela, P.K. Wrona. Some anion-transport properties of Nafion™ 117 from fuel cell hydrogen peroxide generation data, *Journal of Power Sources* **158** (2006) 1262-1269. https://doi.org/10.1016/j.jpowsour.2005.10.019